FF

GSI

GSI-Preprint-95-81
NOVEMBER 1995

COMPARISON OF CHROMOSOMAL DAMAGE INDUCED BY X-RAYS AND Ar IONS WITH AN LET OF 1840 keV/µm IN G1-PHASE V79 CELLS

S. RITTER, E. NASONOVA, M. SCHOLZ, W. KRAFT-WEYRATHER, G. KRAFT

(To be published in Int. J. Radiat. Biol.)

SD 9603

Gesellschaft für Schwerionenforschung mbH
Postfach 110552 · D-64220 Darmstadt · Germany

Comparison of chromosomal damage induced by X-rays and Ar ions with an LET of 1840 keV/μm in G_1-phase V79 cells

S. Ritter#*, E. Nasonova +, M. Scholz#, W. Kraft-Weyrather#
and G. Kraft#

*Author for correspondence

#Biophysik
Gesellschaft für Schwerionenforschung
Planckstr. 1
D-64291 Darmstadt
Germany

+Laboratory of Nuclear Problems
Joint Institute for Nuclear Research
141980 Dubna
Russia

Tel. + +49 6159 712585
Fax + +49 6159 712106

Abstract

Synchronous V79 Chinese hamster cells were exposed in G_1-phase to either X-rays or 4.6 MeV/u Ar-ions (LET: 1840 keV/μm) and the induction of chromosomal damage was measured at 5 sampling times ranging from 14 to 30 hours after treatment. To distinguish between cells in the first and second postirradiation cycle the Fluorescence-plus-Giemsa technique was applied. The experiment showed that the time course of the appearance of damaged cells is markedly influenced by radiation induced cell cycle delays and depends on both radiation quality and dose. The yield of aberrant metaphases and the number of aberrations per metaphase was found to increase with sampling time, but this increase was more pronounced for Ar ions. These differences in the yield time profiles of X-ray and Ar ion induced chromosomal damage are particularly important for an accurate determination of the RBE for particles. Our data clearly indicate that meaningful RBE values can only be obtained, if chromosomal damage is analyzed at several postirradiation sampling times and the complete time course of the expression of chromosomal damage is taken into account. Besides these quantitative differences, differences in the spectrum of chromosomal lesions were observed for X-rays and Ar ions. Following particle exposure more breaks and less exchange-type aberrations were formed compared to X-irradiation and, despite irradiation in G_1-phase, a significant number of chromatid-type aberrations occured in Ar-irradiated samples. The experimental results are interpreted on the basis of the different pattern of energy deposition by sparsely and densely ionizing radiation. In addition, a statistical analysis based on the Neyman type A distribution is performed, which takes into account the specific stochastic properties of particle irradiation.

1. Introduction

In the first chromosome experiment using various light particles Skarsgard et al. (1967) found that the RBE for the induction of chromosome aberrations parallels the RBE for cell inactivation when graphed as a function of the linear energy transfer (LET). Meanwhile inactivation by charged particles has been extensively studied and these investigations show that the RBE or the cross sections for cell inactivation exhibit a more complex structure as function of LET. Individual RBE maxima at increasing LET values are reported for protons, He and heavier ions in order of increasing atomic numbers but with decreasing height (Barendsen et al. 1963, Kraft 1987, Furusawa et al. 1992, Belli et al. 1993). These maxima have been identified as the optimal ionization density for the production of lethal lesions. The steep decline at higher LET values is probably due to a saturation effect (Butts and Katz, 1967, Hall 1988).

The investigation of chromosomal damage provides a deeper insight into the mechanisms of radiation action at the cellular level than inactivation measurements, because this technique allows to detect the number of lesions per cell and their distribution between cells. Also differences in the spectrum of aberration types can be distinguished giving more information about the quality of the molecular lesions induced. However, the interpretation of particle experiments is complicated by pronounced cell cycle perturbations and mitotic delay which interfere more strongly with the expression of chromosomal damage than X-rays (Ritter et al. 1990). Moreover, investigations of Lloyd et al. (1977) and Pyatkin et al. (1984) indicate that cell cycle progression delays are related to the aberration burden of a cell, i.e. cells carrying two aberrations are delayed for longer times than those carrying only one aberration. If this holds true, for high LET radiation, which induces pronounced cell cycle delays (Lücke-Huhle et al. 1979, Collyn-d'Hooghe et al.1981, Scholz et al. 1994) a drastic increase in the frequency of aberrations with sampling time is expected. So far a detailed analysis of high LET induced chromosomal damage in relation to sampling time

has not been made. In general, heavy ion induced chromosomal damage has been scored only once within a period of about one cell generation time (Skarsgard et al. 1967, Edwards et al. 1986, Sabatier et al. 1987, Suzuki et al. 1990, Edwards et al. 1994) or twice, at two widely spaced sampling times (Govorun et al. 1982).

In the experiment described below, the induction of chromosomal damage in V79 Chinese hamster cells by X-rays and 4.6 MeV/u Ar ions as representatives of sparsely and densely ionizing radiation has been analyzed at several postirradiation sampling times. Cells were collected in metaphase between 14 and 30 hours after exposure, a period which corresponds to 2.5 cell generation times of control cells and ensures that also very delayed cells will be included in the analysis. Because the radiosensitivity varies within the cell cycle (Dewey et al. 1970, Durante et al. 1994 and references therein), the experiments were performed with synchronous cells. In addition, the Fluorescence-plus-Giemsa technique was applied to differentiate between cells in the first and second postirradiation mitosis. Recently a brief summary of some of the results has been reported (Ritter et al. 1994).

2. Materials and Methods

2.1. Cell culture

V79 Chinese hamster cells with a modal chromosome number of 22 and a cell generation time of 12 h were used in this study. The cells were cultivated according to standard procedures as previously reported (Ritter et al. 1990). For the experiments cells were synchronized in G_1-phase by centrifugal elutriation (J2-21M/E centrifuge, Beckmann) and seeded in Petri dishes at a density of $1x10^5$-$2x10^5$ cells/dish depending on harvesting time and radiation dose. Two hours after seeding, when the cells were attached and spread, samples were irradiated with Ar ions or X-rays.

2.2. Irradiation

The exposure to 4.6 MeV/u Ar ions (LET 1840 keV/μm) was performed at the UNILAC (GSI, Darmstadt, Germany) as described by Kraft et al. (1980). The delivered fluences of $1x10^6$ and $4x10^6$ particles/cm^2 correspond to a dose of 2.9 and 11.7 Gy, respectively. The exposure of cells to 2, 4 and 7 Gy X-rays was done with a Siemens therapeutic X-ray machine operated at 250 kV and 20 mA with a 1mm Cu and a 1mm Al filter. To diminish experimental variation, both exposures were performed in parallel, i.e. at the same time with the same fraction of cells. Flow cytometric measurements confirmed that 95% of cells were in G_1-phase during irradiation.

2.3 Fluorescence-plus-Giemsa technique

In order to differentiate between metaphases in the first and second cell generation the Fluorescence-plus-Giemsa technique according to Perry and Wolff (1974) was applied with minor modifications. In brief, 10μg/ml BrdU were added immediately after irradiation and the samples were kept in the dark at 37^{o}C until fixation. Cells were harvested 14, 18, 22, 26 and 30 hours after irradiation. 2 hours before fixation 0.1 μg/ml colcemid was added to the samples to accumulate mitotic cells. Chromosome preparations were made according to standard techniques: Cells were trypsinized, treated with hypotonic solution (0.075M KCl) and fixed with methanol-acetic acid (3:1). All procedures up to the fixation of cells were performed under subdued light to avoid the photolysis of BrdU, which causes the formation of additional DNA breaks. Fixed cells were dropped on wet, ice-cold slides and air-dryed. Slides were incubated in Hoechst 33258 solution (1μg/ml), irradiated for 1 hour with a low-pressure UV-lamp (λ 365nm) and stained with 3% Giemsa in phosphate buffer (pH 6.8). As a result, the

chromosomes of first postirradiation mitoses are darkly stained, second generation mitosis show "harlequin" chromosomes.

2.4 Chromosome analysis

The percentage of aberrant cells and the aberration types were seperately determined for first and second cycle metaphases. Chromosome aberrations were classified according to Savage (1975). Gaps were not counted as aberrations. In the case of a dicentric chromosome or a centric ring one acentric fragment was subtracted from the number of fragments present in the cell. The data, based on the analysis of one hundred aberrant first or second cycle metaphases per dose and sampling time, are summerized in table 1. Also, the mitotic index was determined for each sample by the direct scoring of a population of 1000-2000 cells on the slides (tab. 1 and fig. 1).

Measurement of the cell survival shows that the delivered particle fluences of 1×10^6 and 4×10^6 particles/cm^2 correspond to survival levels of 70 and 20%, the exposure to 2, 4 and 7 Gy of X-rays result in 80, 45 and 15% cell survival, respectively.

2.5 Statistical analysis

Errors on the proportion of mitotic cells and aberrant metaphases plotted in figures 1 and 2 are standard deviations of a binominal distribution

$$\Delta F = \sqrt{\frac{F(1-F)}{N}},$$

where F is the number mitotic cells or aberrant metaphases and N the total number of cells scored. The statistical uncertainty of the measured number of aberrations/metaphase (fig. 3), the frequency of chromatid type aberrations (fig. 4) and chromosomal breaks (fig. 5) was calculated by $\sqrt{n}$, where n is the frequency under consideration.

The distribution of chromosomal aberrations within a cell population was investigated by means of two different stochastic distributions: the Poisson distribution and the Neyman type A distribution.
The Poisson distribution is given by

$$p(j, \bar{n}) = \frac{\bar{n}^j}{j!} e^{-\bar{n}}$$

where j is the number of aberrations per individual cell and $\bar{n}$ is the average number of aberrations per cell in the population.

The Neyman type A distribution is a generalized Poisson distribution given by

$$p(j) = e^{-\bar{n}_1} \frac{\bar{n}_2^j}{j!} \sum_{k=0}^{\infty} \frac{k^j}{k!} \left(e^{-\bar{n}_2} \bar{n}_1\right)^k$$

which takes into account the stochastic distribution of particle traversals as discussed by Virsik and Harder (1981). Here, $\bar{n}_1$ can be interpreted as the average number of particle traversals per nucleus, whereas $\bar{n}_2$ represents the average number of aberrations per particle traversal through the nucleus.
Fits to the experimental data were performed using the 'GD' display and fit software package available for UNIX workstations at GSI. The fit routines are based on algorithms given in Bevington (1969).

3. Results

3.1. Mitotic delay

The fraction of cells reaching mitosis as a function of time after the exposure of G_1-phase cells are listed in table 1 and plotted in figure 1. Furthermore, in table 1 the percentage of first and second postirradiation metaphases is given. Unirradiated control cells complete their first mitosis by 14 h or slightly earlier, whereas X-ray and Ar ion irradiation prolong the cell cycle progression and delay the entry of cells into mitosis. The duration of this delay increases with dose or particle fluence. However, there is a significant difference between X-ray and particle irradiation: Cells exposed to X-rays proceed in a synchronous wave through the first postirradiation cell cycle as indicated by a steep rise and fall in the number of mitotic cells within a few hours. Higher doses shift this peak to later sampling times (fig. 1). The synchrony of X-irradiated cells is also largely maintained during the second postirradiation cycle as indicated by the measurements 26 and 30 hours after treatment. In contrast, after heavy ion exposure the differences between minimum and maximum values of the mitotic index are diminished indicating a fast desynchronisation of the cell population. This finding is confirmed by means of the Fluorescence-plus-Giemsa technique, which shows a pronounced spread of first cycle metaphases following Ar ion exposure resulting in a mixture of cell generations at late sampling times (tab. 1).

3.2. Frequency of aberrant metaphases in relation to sampling time

In order to quantify the chromosomal damage induced by X-rays and Ar ions the percentage of aberrant metaphases was determined at 5 successive sampling times starting from 14 up to 30 hours after exposure. The data show that the amount of aberrant first and second generation mitoses varies with time and follows a different time course for both radiation types (tab. 1 and fig. 2): 14 hours after X-ray exposure the amount of abnormal first cycle metaphases is already as high as 28, 48 and 78% for 2, 4 and 7 Gy, respectively. This percentage rises slightly with time. In contrast, after the exposure of cells to 1×10^6 and 4×10^6 Ar ions/cm^2 corresponding to doses of 2.9 and 11.7 Gy, the number of damaged first cycle metaphases amounts only to 14 and 19% at the first sampling time. Then, their frequency increases more steeply with sampling time than it was found for X-rays and by 22 to 26 hours after Ar-exposure only aberrant metaphases are seen. Furthermore, following particle exposure the frequency of aberrant mitoses increases less with dose than it was found for X-rays.

A significant amount of second cycle metaphases appears 26 hours after exposure (fig. 2 and tab. 1). The limited data, which are available for this cell generation indicate that the appearance of damaged second cycle metaphases follows in general the same tendency found for first generation cells: For X-rays a high amount of damaged second cycle metaphases is already present at the onset of the second cycle increasing slowly with time, whereas for particles a low amount of damaged second cycle metaphases is observed increasing steeply with time. However, for both radiation types the percentage of aberrant metaphases decreases with cell generation.

3.3. Aberration frequency and spectrum of aberration types with respect to sampling time

Differences in the induction of chromosomal damage by sparsely and densely ionizing radiation become most evident, when the aberration frequency and the spectrum of aberration types are compared. For both radiation types an increase in the number of aberrations per cell with sampling time is observed in first and second cycle metaphases (fig. 3). However, this rise is less pronounced for sparsely ionizing

radiation. For example, in X-irradiated samples the aberration frequency increases in first cycle metaphases by a factor of 3, in Ar ion irradiated samples however by a factor of 20. Second generation cells follow in general the same trend, but due to the limited number of data available for the second generation the increase with time cannot be precisely determined in this experiment. Furthermore, in X-irradiated samples the number of aberrations per cell rises proportional to applied dose, i.e. doubling the dose yields about twice as many aberrations per cell at a given sampling time. This is not the case for particle exposure, where the number of aberrations doubles, when the dose or the particle fluence is increased by a factor of 4.

When the spectrum of aberration types observed in first cycle metaphases (tab. 1) is analyzed an unexpected high amount of chromatid-type aberrations (chromatid breaks and chromatid exchanges) is found in Ar-irradiated samples (fig. 4). Despite the fact that 95% of the cells were in G_1-phase at the time of exposure about 30 to 35% of all lesions, which are induced by Ar ions are chromatid-type aberrations. In contrast, in X-irradiated samples only 10 to 15% of all lesions in first cycle metaphases are chromatid-type aberrations (fig. 4). These rates remain relatively constant for each radiation type and vary only slightly with dose or sampling time. Only in very delayed X-irradiated cells reaching the first postirradiation mitosis 26 h after exposure the amount of chromatid-type aberrations increases to the level observed after Ar irradiation. In second cycle metaphases the frequency of chromatid-type aberrations is nearly the same following X-rays and Ar ion irradiation, i.e. for both radiation types a rate of about 30% of chromatid-type aberrations are found.

When the aberration-types are classified as chromosomal breaks and exchange-type aberrations, another significant difference in the distribution of aberration-types is observed in first cycle metaphases. Chromosomal breaks include chromosome- and chromatid-type breaks, exchange-type aberrations comprise dicentrics, centric rings and all other aberration-types listed in table 1. As shown in figure 5 after Ar-exposure at least 50% of aberrations detected in first division cells belong to the category of chromosomal breaks. Although the yield of particle induced aberrations increased drastically with harvesting time (fig. 3) the percentage of chromosomal breaks remained nearly the same up to 30 h after irradiation. After X-ray exposure the percentage of chromosomal breaks is much lower. Most lesions are exchange-type aberrations. Only very delayed X-irradiated cells entering the first postirradiation mitosis by 26 hours contain a high amount of breaks. For second cycle metaphases the difference in the rate of chromosomal breaks versus exchange-type aberrations disappears due to an increase in the percentage of breaks in X-irradiated cultures and a decrease in particle irradiated cultures (see tab. 1).

3.4. Frequency of aberrations per cell

In the case of X-ray induced chromosomal damage the relative frequencies of aberrations per individual metaphase measured at a given sampling time are well described by the Poisson distribution (data not shown). The particle exposure data were additionally fitted by a Neyman type A distribution, a generalized Poisson distribution which takes into account the stochastic distribution of particle traversals as well as the stochastic distribution of aberrations induced by a single particle traversal. This distribution for the description of aberration frequencies after charged particle irradiation was proposed by Virsik and Harder (1981). In general, the Neyman type A distribution yields a better description of the experimental data than the Poisson distribution as shown in figure 6 for the relative frequencies of aberrations per individual metaphase 18h and 22h after Ar exposure. The corresponding fit parameters are listed in table 2. Major discrepancies between the two distributions are observed in particular for the cells with no aberrations. In addition, the experimental data show the typical overdispersion, i.e. the width of the distribution is broader than expected from a pure Poisson distribution with the same mean value.

4. Discussion

4.1. Spatial energy deposition by sparsely and densely ionizing radiation

The observed differences in the response of cells to sparsely and densely ionizing radiation are related to the spatial energy distribution by both radiation types. When X-rays are applied, the cell nucleus is homogeneously covered by energy depositions within the limits as defined by microdosimetry, so that all cells are potentially at risk for the formation of aberrations. In the case of low energy particles however, the dose is extremely inhomogeneously deposited concerning both, the dose distribution inside each particle track and the number of the particle traversals per cell nucleus. Tracks of 4.6 MeV/u Ar ions have a diameter of about 2 μm. Within the track the dose increases from about 0.2 Gy at the outer parts to several hundred kGy in the center (Kraft et al. 1992). Due to the low particle fluences, pronounced stochastic fluctuations in the number of particle traversals per cell nucleus occur, and the probability for an overlap of tracks is very small because the track radii are small at low energies.

For V79 G_1-phase cells synchronized by centrifugal elutriation and plated as described above the mean geometrical cross section of the cell nucleus is approximately 50μm^2 (Scholz 1992). Therefore, for fluences of $1x10^6$ and $4x10^6$ particles/cm^2 a mean number of 0.5 and 2 particle traversals per cell nucleus are calculated. From Poisson statistics it follows that a mean value of 0.5 traversals corresponds to 60% of cell nuclei which received no particle hit, 30% are hit once, 7.5% are hit twice and 2.5% of the nuclei are hit three times or more. For a mean value of 2 traversals these frequencies change to 14, 27, 27 and 32%, respectively. Consequently, cells with nuclei that are not in the path of particle tracks will not develop aberrations at all, whereas those that are traversed are at risk for the formation of aberrations. The numbers derived above have to be taken as a rough estimate to illustrate the importance of stochastic effects for the interpretation of the data. For a more detailed comparison, the radial extension of the track and the radial dose distribution inside the track have to be taken into account. Thus, although the exposure to $1x10^6$ and $4x10^6$ Ar ions/cm^2 corresponds to doses as high as 2.9 and 11.7 Gy, the dose deposition per cell nucleus is extremely heterogeneous.

In the following, the biological consequences of the nonuniformity of energy deposition by particle exposure are discussed: (a) the influence of the inhomogenous dose distribution inside the tracks that affects the spectrum of the aberration types, (b) the influence of the stochastic fluctuations in the number of particle traversals per cell that affect the time course of the appearance of chromosomal damage; and, (c) importance of the implications of (b) for the calculation of the relative biological efficiency.

4.2. Ratio of chromosomal breaks versus exchange-type aberrations

The comparison of the aberration types induced by both radiation types shows (fig. 5) that densely ionizing radiation induces a much higher frequency of chromosomal breaks than sparsely ionizing radiation. Similar results were obtained in previous experiments, where chromosomal damage was scored either in mitotic cells with conventional cytogenetic techniques (Govorun et al. 1982, Edwards et al. 1986, Ritter et al. 1990, Durante et al. 1994) or by the premature chromosome condensation technique (Suzuki et al. 1990, Goodwin et al. 1994) which allows visualization of chromosomal damage in interphase cells.

The observed alterations in the ratio of chromosomal breaks versus exchange-type aberrations indicate that the initial molecular damage from high LET radiation is

qualitatively different from low LET damage. The lesions produced by particle tracks seem to be more severe and therefore less repairable. Evidence supporting this assumption comes from two sources. First, DNA rejoining studies have demonstrated that the fraction of residual DNA damage increases with LET (Aufderheide et al. 1987, Heilmann et al. 1993, Weber and Flentje 1993, Rydberg et al. 1994). A pronounced lack of rejoining was already observed in cells exposed to O ions with an LET value of 285 keV/μm (Aufderheide et al. 1987). Second, modelling studies predict a gradual change in the molecular spectrum of lesions with increasing LET, in particular a rise in the ratio of multiple to single damage as recently reviewed (Prise 1994).

4.3. Induction of chromatid-type aberrations

It is generally assumed that the main type of aberrations induced by radiation in G_1-phase cells is the chromosome type, which involves both chromatids of a chromosome at the same location, whereas in S- or G_2-phase mainly chromatid-type aberrations are formed that affect only one chromatid (Evans 1962, Savage 1975). In our experiments, where at the time of exposure 95% of cells were in G_1-phase and only 5% in early S-phase an unexpected high amount of about 30-35% of chromatid-type aberrations has been observed after Ar- but not after X-irradiation (fig. 4).

At almost all sampling times after X-irradiation only 10-15% of all chromosomal lesions are chromatid-type aberrations. This is consistent with data from Dewey et al. (1970) and Tremp (1981) for other Chinese hamster cell lines exposed in G_1-phase. Only in very delayed X-irradiated cells, which reached mitosis by 26 hours we found an increase in the frequency of chromatid-type aberration. Tremp (1981) studied the variation in the amount of damaged cells with harvesting time and observed the same effect.

The much higher rate of chromatid-type aberrations found after particle exposure cannot be attributed to a higher frequency of S- or G_2-phase cells in this experiment, because Ar- and X-irradiation were performed in parallel (see materials and methods). Also, our observation that both chromosome and chromatid-type aberrations were generally found within one cell confirms that almost all chromatid-type aberrations are induced in G_1-phase cells. Obviously, the frequency of chromatid-type aberrations among the total number of aberrations depends strongly on radiation quality. Further evidence for this assumption comes from Sevankajev et al. (1975), who found a higher rate of chromatid-type aberrations in human lymphocytes after neutron irradiation than after X-ray exposure.

Chromatid-type aberrations observed after irradiation of G_1-phase cells are obviously not generated by DNA double strand breaks. Double strand breaks directly induced in G_1-phase cells, would lead to chromosome type aberrations (Evans 1962, Savage 1975). Alkali-labile sites or single strand breaks induced in G_1-phase cells would give rise to chromatid-type aberrations. When unrepaired throughout G_1-phase they can be converted into double strand breaks during S-phase and expressed as chromatid-type aberrations in the subsequent mitosis. This assumption is supported by the finding of Roots et al. (1990) that alkali labile-sites are formed at a higher rate as LET increases. Furthermore, these authors have some evidence that in contrast to X-irradiation a substantial number of single strand breaks remained unrejoined after high LET radiation. Thus, the elevated frequency of chromatid-type aberrations observed in the first postirradiation mitosis after exposure to Ar ions with an LET of 1840 keV/μm can be regarded as a further indication that high LET induced DNA lesions are qualitatively different from those induced by low LET radiation.

4.4. Mitotic delay and cell cycle perturbations

Delay of cell cycle division induced by radiation is a well known and widely demonstrated phenomenon (Lloyd et al. 1977, Lücke-Huhle et al. 1979, Purrot et al.1980, Collyn-d'Hooghe et al. 1981, Pyatkin et al. 1984, Ritter et al. 1990, Scholz et al. 1994). As shown in figure 1 after X-irradiation cells are homogeneously slowed down and the synchrony of the exposed cell population is largely maintained (tab. 1), an observation which agrees well with data obtained for human lymphocytes by the FPG-technique (Purrot et al. 1980) or for synchronous V79 cells by flow cytometry (Scholz et al.1994). In contrast, after particle exposure large variations in the delay of individual cells have been observed as indicated by the kinetics of the mitotic index and the pronounced spread of first cycle metaphases (table 1). Similar variations in the progression delay have been observed by flow cytometry (Scholz et al. 1994). As pointed out above, in the case of particle exposure a differential delay is expected, because unirradiated as well as cells passaged by one or more particles are present within the cell population. Cells, which are not hit progress like control cells, whereas for cells, which are hit, the delay is correlated to the number of particle traversals per nucleus (see tab. 2). In consequence, cell synchrony is rapidly lost after particle exposure. In other words, the fast desynchronization observed after Ar-irradiation is due to the stochastics of particle traversals and will be similar for all low energy, high LET particles.

4.5. Yield of particle induced chromosomal damage

The non-doseproportional yield of aberrant cells induced by Ar ion irradiation also can be explained on the basis of Poisson statistics: Cell nuclei that are not traversed by particles will not develope aberrations. The small fraction of nuclei that are not in the direct path of a particle, but receive ionizations from the outer part of a particle track is negligible at the low particle energy used. For a fluence of $1x10^6$ particles/cm^2 only 40% of the nuclei are hit, whereas for a fluence of $4x10^6$ particles/cm^2 more than 80% of the nuclei are traversed. This means that although the average fluence and therefore the dose is raised by a factor of four, the number of cells which are at risk for the formation of aberrations only doubles. In accordance, the amount of aberrations per cell doubles as shown in fig. 3. Therefore, increasing the particle fluence from $1x10^6$ to $4x10^6$ particles/cm^2 increases the number of cells traversed by particles by a factor of two and the amount of aberrations by a factor of two.

4.6. Frequency of aberrations per cell

Statistical analysis of the frequency of aberrations per individual metaphase cell clearly showed that for Ar ion exposure the experimental data are better described by the Neyman type A distribution than by the Poisson distribution as proposed by Virsik and Harder (1981). The Neyman type A distribution has been also used by Durante et al. (1994) for investigations of chromosome aberrations after α-particle irradiation. In contrast to our analysis, they fixed the average number of particle traversals according to the size of the cells and the particle fluence used for the experiments. This is not justified, however, if cell cycle delays are correlated with the aberration burden of the cells. Obviously, the cells with a low number of particle traversals and correspondingly low chromosomal damage will become visible in mitosis earlier than the cells with a high number of traversals and a correspondingly more severe delay, so that the distribution of particle traversals will be distorted at late sampling times compared to the initial distribution. This is supported by the comparison of fit parameters given in table 2. For example, for irradiation with 4×10^6part./cm^2 there is a very strong increase of $\overline{n_1}$, representing the average number of traversals, with time, whereas $\overline{n_2}$, denoting the average number of aberrations

per traversals, remains nearly constant within the errors. Thus, the fit parameters clearly reflect the damage dependent cell cycle delays.

4.7. The relative biological efficiency

In a large number of experiments the comparision of chromosomal damage induced by sparsely and densely ionizing radiation was based on the amount of lesions scored at only one (Skarsgard et al. 1967, Edwards et al. 1986, Sabatier et al. 1987, Suzuki et al. 1990, Edwards et al. 1994) or two widely spaced sampling times (Govorun et al. 1982). However, data are inconsistent and the reported RBE values differ considerably. For example, for low energy particles (N, O, Ne) with LETs in the range of 350 to 530 keV/μm published RBE values vary between 0.2 (Suzuki et al. 1990, Edwards et al. 1994) and 1.5 (Skarsgard et al. 1967). The discrepancy observed in these experiments can be related to the fact that the samples used for aberration detection are not representative for the whole population.

As shown before cell cycle perturbations and mitotic delay strongly influence the time course of the expression of chromosomal damage and cells collected at only one sampling time after irradiation do not represent the initial distribution of damage. From figures 2 and 3 it is most evident that at early sampling times X-ray induced lesions predominate, wheras at later sampling times particle induced aberrations are found more frequently. Consequently, RBE values smaller than one will result from the comparison of chromosomal damage at early sampling times used in most particle experiments, but RBE values greater than 1 will be obtained at the late sampling times. Therefore, in particle experiments many sampling times should be used in order to cover the whole spectrum of particle induced damage corresponding to the initial stochastic distribution of particle traversals. A novel approach for the estimation of a realistic RBE value for the induction of chromosome damages, which is based on the integration of the chromosome damages over the total sampling time interval will be described in a separate paper.

In conclusion, our study provides further evidence of a significant difference in the nature of particle and X-ray induced lesions that manifests at cellular level in the cell cycle kinetics, the spectrum of aberration types and the distribution of aberrations among the cells. From the data presented here a firm conclusion on the intrinsic nature of high LET lesions cannot be made. This needs more systematic studies covering a larger spectrum of particles and LET values. Meanwhile further experiments with low energy particles with LET values of 400 keV/μm and 4000 keV/μm have been performed and are currently under investigation.

Acknowledgement

The authors acknowledge W. Becher and G. Lenz for their excellent technical support during irradiation and E. Kehr for her skillful assistance in preparing the cells. This work was partly supported by CEC, Brussels, under contract no. F13P CT92 0064 and DARA, Bonn, under contract no. 50WB 93120-4-ZK.

References

Aufderheide, E., Rink, H., Hieber L. and Kraft, G., 1987, Heavy ion effects on cellular DNA: strand break induction and repair in cultured diploid lens epithelian cells. International Journal of Radiation Biology, **51**, 779-790.

Barendsen, G., H., Walter, H., M., D., Fowler, J., F. and Bewley D., K., 1963, Effects of different ionizing radiations on human cells in tissue culture. III: Experiments with cyclotron accelerated alpha-particles and deuterons. Radiation Research, **18,** 106-119.

Belli, M., Cera, F., Cherubini, R., Haque, A., M., I., Ianzini, F., Moschini, G., Sapora, O., Simone, G., Tabocchini, M., A. and Tiveron, P., 1993, Inactivation and mutation induction in V79 cells by low energy protons: re-evaluation of the results at the LNL facility. International Journal of Radiation Biology, **63,** 331-337.

Bevington, P.,R., 1969, Data reduction and error analysis for the physical science (Mc Craw Hill, New York).

Butts, J., J. and Katz, R., 1967, Theory of RBE for heavy ion bombardment of dry enzymes and viruses. Radiation Research **30,** 855-879.

Collyn-d'Hooghe, M., Hemon D., Gilet, R., Curtis, S., B., Valleron, A. J. and Malaise, E., P., 1981, Comparative effects of ^{60}Co γ-rays and neon and helium ions on cell cycle duration and division probability of EMT 6 cells. A time-lapse cinematography study. International Journal of Radiation Biology **39,** 297-306.

Dewey, W., C., Furman, S., C. and Miller, H., H., 1970, Comparison of letality and chromosomal damage induced by X-rays in synchronized Chinese hamster cells in vitro. Radiation Research, **43,** 561-581.

Durante, M., Gialanella, G., Grossi, G., F., Nappo, M., Pugliese, M., Bettega, D., Calzolari, P., Chiorda, G., N., Ottolenghi, A. and Tallone-Lombardi, L., 1994, Radiation-induced chromosomal aberrations in mouse 10T1/2 cells: dependence on the cell-cycle stage at the time of irradiation. International Journal of Radiation Biology, **65,** 437-447.

Edwards, A., A., Lloyd, D., C., Prosser, J., S., Finnon, P. and Moquet, J., E., 1986, Chromosome aberrations induced in human lymphocytes by 8.7 MeV protons and 23.5 MeV helium-3 ions. International Journal of Radiation Biology, **50,** 137-145.

Edwards, A.,A., Finnon, P., Moquet, J.,E., Lloyd, D.,C., Darroudi, F., and Natarajan, A., T.,1994, The effectiveness of high energy Neon ions in producing chromosomal aberrations in human lymphocytes. Radiation Protection Dosimetry, **52,** 299-303.

Evans, H., J., 1962, Chromosome aberrations induced by ionizing radiations. In: International Review of Cytology. Volume 13. Edited by: G. H. Bourne and J. F. Danielli. (Academic Press, New York), pp. 221-321.

Furusawa, Y., Fukutsu, K., Itsukaichi, H., Eguchi-Kasai, K., Ohara, H., Yatagai, F. and T. Kanai, 1992, Biological effectiveness by the different heavy ion species with the same LET. In: Proceedings of the second workshop on physical and biological research with heavy ions. Edited by: K. Ando and T. Kanai, NIRS report NIRS-M-90, HIMAC-003, Chiba, Japan, pp.11-13.

Goodwin, E., H., Blakely, E., A. and Tobias, C., A., 1994, Chromosomal damage and repair in G_1-phase Chinese hamster ovary cells exposed to charged particle beams. Radiation Research, **134,** 343-351

Govorun, R., D., Ryzhov, N., I., Smirnova, O., A., Portman, A., I., Erzgraber, G. and Eichhorn, K., 1982, Effect of heavy ions on mammalian cells. Radiobiologya, **22**, 648-653.

Hall, E., J., 1988, Radiobiology for the radiologist, third edition (J. B. Lippincott Company, Philadelphia).

Heilmann, J., Rink, H., Taucher-Scholz, G. and Kraft, G., 1993, DNA strand break induction and rejoining and cellular recovery in mammalian cells after heavy ion irradiation. Radiation Research, **135**, 46-55.

ISCN, 1978, An international system for human cytogenetic nomenclature. Cytogenetics and Cell Genetics. **21**, 309-404.

Kraft, G., 1987, Radiobiological effects of very heavy ions: Inactivation, induction of chromosome aberrations and strand breaks. Nuclear Science Application, **3**, 1-28.

Kraft, G., Daues, H. W., Fischer, B., Kopf, U., Leibold, H. P., Quis, D., Stelzer, H., Kiefer, J., Schopfer, R., Schneider, E., Weber, U., Wulf, H. and Dertinger, H., 1980, Irradiation chamber and sample changes for biological samples. Nuclear Instruments and Methods, **168**, 175-179.

Kraft, G., Krämer, M. and Scholz, M., 1992, LET, track structure and models, A review. Radiation and Environmental Biophysics, **31**, 161-180.

Lloyd, D., C., Dolphin, G. W., Purrot, R. J. and Tipper P. A., 1977, The effect of X-ray induced mitotic delay on chromosome aberration yields in human lymphocytes. Mutation Research, **42**, 401-412.

Lücke-Huhle, C., Blakely, E.A., Chang, P., Y. and Tobias, C. A., 1979, Drastic G_2 arrest in mammalian cells after irradiation with Heavy-ion beams. Radiation Research **79**, 97-112.

Perry, P. and Wolff S., 1974, New Giemsa method for the differential staining of sister chromatids. Nature, **251**, 156-158.

Prise, K.,M., 1994, Use of radiation quality as a probe for DNA lesion complexity. International Journal of Radiation Biology, **65**, 43-48.

Purrott, R. J., Vulpis, N. and Lloyd, D. C., 1980, The use of harlequin staining to measure delay in the human lymphocyte cell induced by in vitro X-irradiation. Mutation Research, **69** ,275-282.

Pyatkin, E. K., Nugis V. U., Pokroskaya, V. N., 1984, Proliferative activity and frequency of chromosome aberrations during the first mitosis in 50-, 60- and 70-h-cultures of irradiated lymphocytes and in mixed cultures of irradiated and nonirradiated cells. Radiobiologya, **24**, 310-314.

Ritter, S., Kraft-Weyrather, W., Scholz, M. and Kraft G., 1990, Influence of radiation quality on heavy ion induced chromosome aberrations in V79 cells. Radiation Protection Dosimetry, **31**, 257-260.

Ritter, S., Nasonova, E., Kraft-Weyrather, W. and Kraft, G., 1994, Influence of radiation quality on the expression of chromosomal damage. International Journal of Radiation Biology, **66**, 625-628.

Roots, R., Holley, W., Chaterjee, A., Irizarry, M. and Kraft, G., 1990, The formation of strand breaks in DNA after high-LET irradiation: a comparison of data from in vitro and cellular systems. International Journal of Radiation Biology, **58**, 55-69.

Rydberg, B., Löbrich, M and Cooper, P.,K., 1994, DNA double- strand breaks induced by high erergy neon and iron ions in human fibroblasts. I. Pulsed-field gel electrophoresis method. Radiation Research, **139**, 133-141.

Sabatier, L., Al Achkar, W., Hoffschir, F., Luccioni, C. and Dutrillaux, B., 1987, Qualitative study of chromosomal lesions induced by neutrons and neon ions in human lymphocytes at G_0-phase. Mutation Research, **178**, 91-97.

Savage, J., R., K., 1975, Classification and relationships of induced chromosomal structural changes. Journal of Medical Genetics, **12**, 103-122.

Scholz, M., 1992, Zellzyklusverzoegerungen synchroner Zellpopulationen nach Schwerionenbestrahlung. PhD thesis, University of Heidelberg, FRG, GSI Report 92-28.

Scholz, M., Kraft-Weyrather, W., Ritter, S. and Kraft, G., 1994, Cell cycle delays induced by heavy on irradiation of synchronous mammalian cells. International Journal of Radiation Biology, **66**, 59-75.

Sevankajev, A., V., Zherbin, E. A., Luchnik, N.,N., Obaturov, G., M., Kozlov, V., M., Tatte, E., G., and Kapchigashev S., P., 1979, Genetical effects induced by neutrons in human peripheral blood lymphocytes in vitro. Genetika, **15**, #6, 1046-1060.

Skarsgard, L. D., Kihlman, B. A., Parker, L., Pujara, C. M. and Richardson, S., 1967, Survival, chromosome abnormalties, and recovery in heavy-ion- and x-irradiated mammalian cells. Radiation Research Supplement, **7**, 208-221.

Suzuki, K., Suzuki, M., Nakano, K., Kaneko, I. and Watanabe M., 1990, Analysis of chromatid damage in G_2-phase induced by heavy ions and X-rays. International Journal of Radiation Biology, **58**, 781-789.

Suzuki, M., Watanabe, M., Suzuki, K., Nakano, K. and Matsui, K., 1992, Heavy ion induced chromosome breakage studied by premature chromosome condensation (PCC) in Syrian hamster embryo cells. International Journal of Radiation Biology, **62**, 581-586.

Tremp, J., 1981, Chromosome aberrations and cell survival in irradiated mammalian cells. Radiation Research, **85**, 554-566.

Virsik, R., P. and Harder, D., 1981, Statistical interpretation of the overdispersed distribution of radiation induced dicentric chromosomes aberrations at high LET. Radiation Research, **85**, 13-23.

Weber, K., J. and Flentje, M., 1993, Lethality of heavy ion-induced DNA double-strand breaks in mammalian cells, International Journal of Radiation Biology, **64**, 169-178.

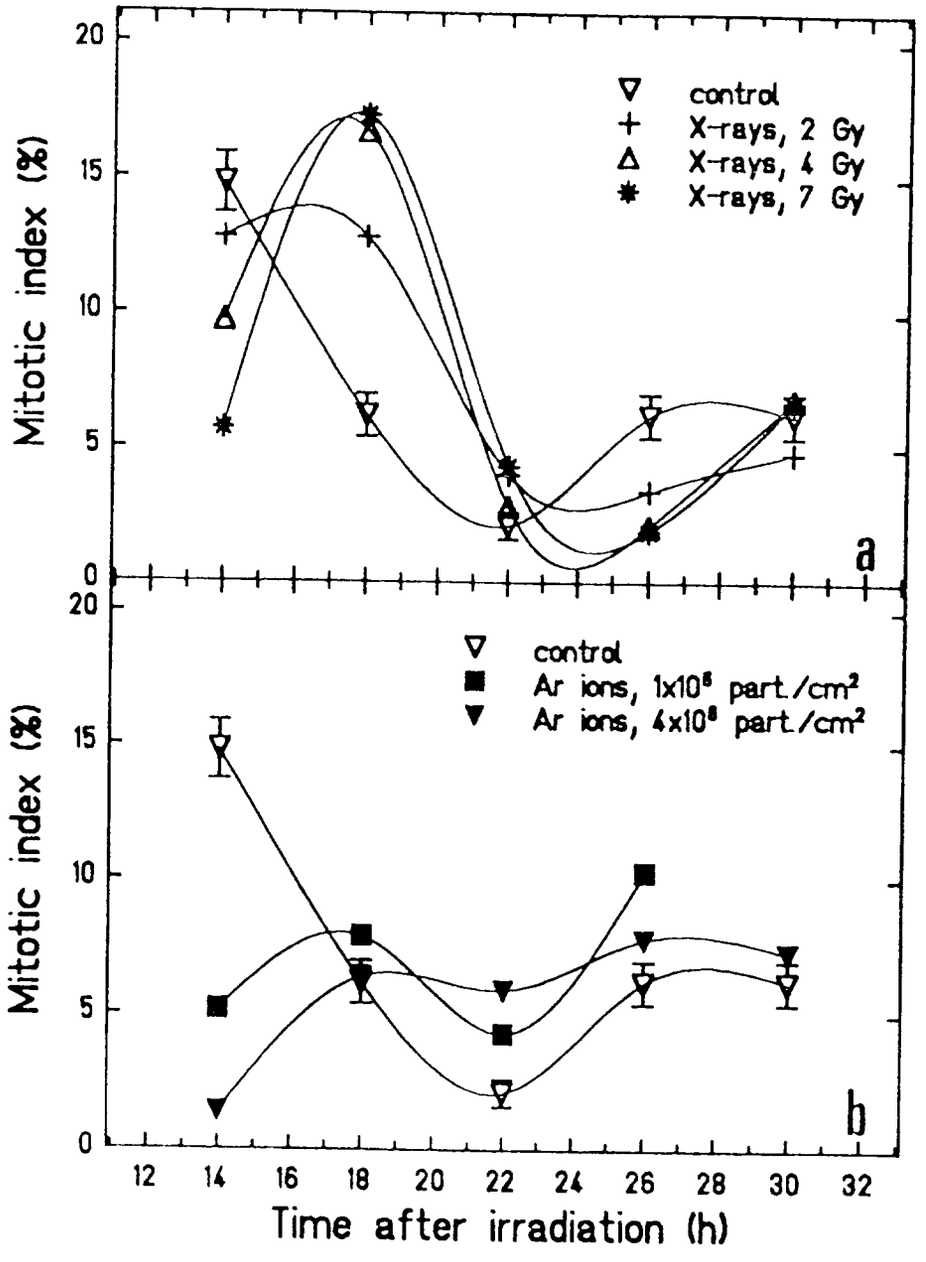

Fig. 1
Mitotic indices found after 2 hour colcemid accumulation periods following irradiation of V79 cells with (a) X-rays or (b) Ar ions in G_1-phase. Frequencies are plotted to the endpoints of the sampling times. Errors on the proportion of mitotic cells were plotted only for one curve but otherwise omitted for clarity (redrawn from Ritter et al. 1994).

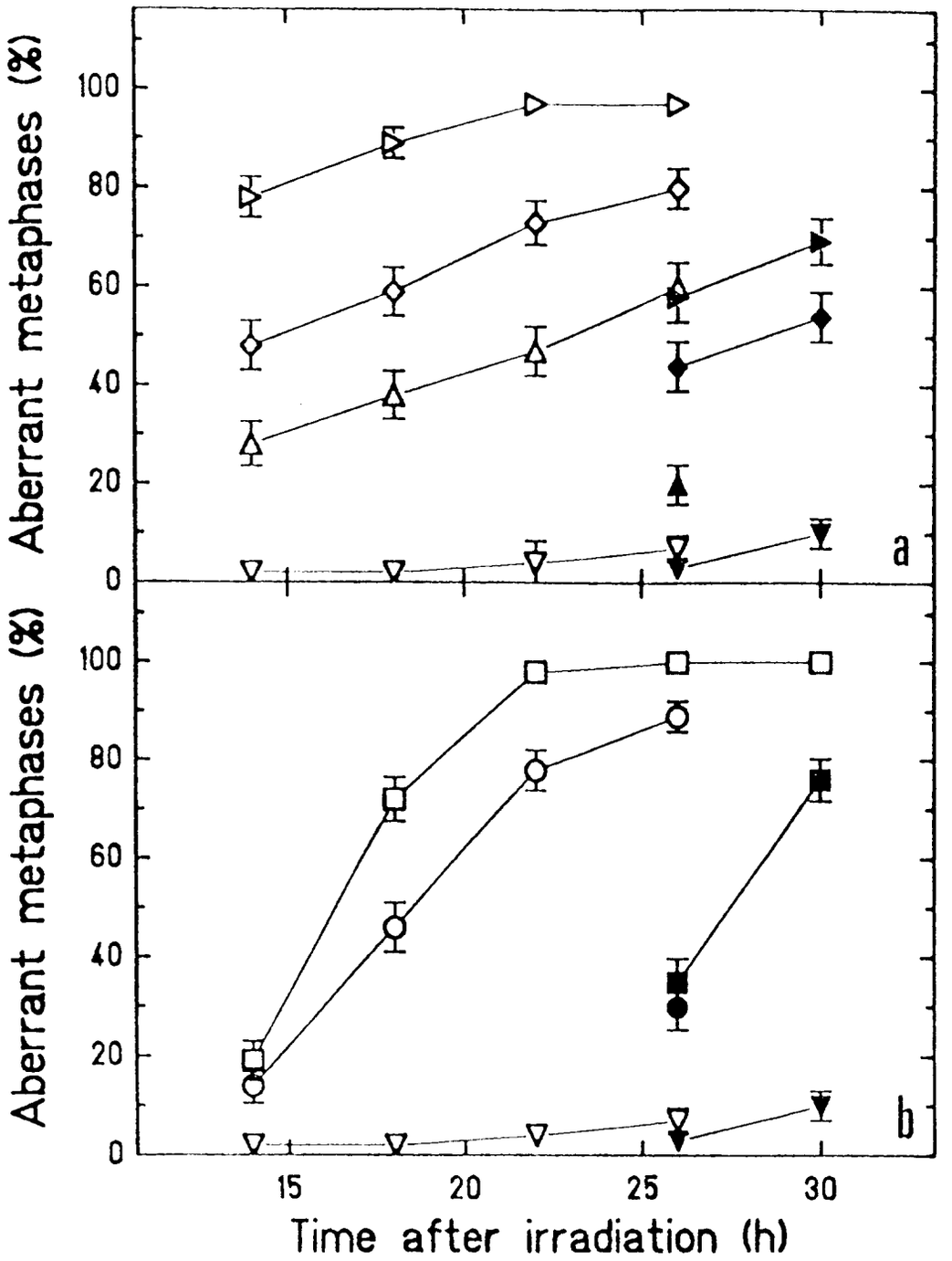

Fig. 2
Percentage of aberrant first and second cycle metaphases observed at different sampling times after the exposure of V79 G_1-phase cells to (a) X-rays and (b) Ar ions. Cells were irradiated at t = 0, treated with BrdU and harvested following 2h incubation in colcemid. Frequencies are plotted to the endpoints of the sampling times. Data are taken from table 1. The open symbols show the data for first cycle metaphases; the solid symbols represent the data for second cycle metaphases.
Fig. 2a: ∇/▼ unirradiated control, Δ/▲ X-rays, 2 Gy, ◇/◆ X-rays, 4 Gy, ▷/▶ X-rays, 7 Gy. Fig. 2b: ∇/▼ unirradiated control, data as in fig. 2a, ○/● Ar ions, $1x10^6$ particles/cm^2, □/■ Ar ions, $4x10^6$ particles/cm^2. Errors on the proportion of aberrant metaphases were determined as described in materials and methods. If absent error bars are too small to be shown.

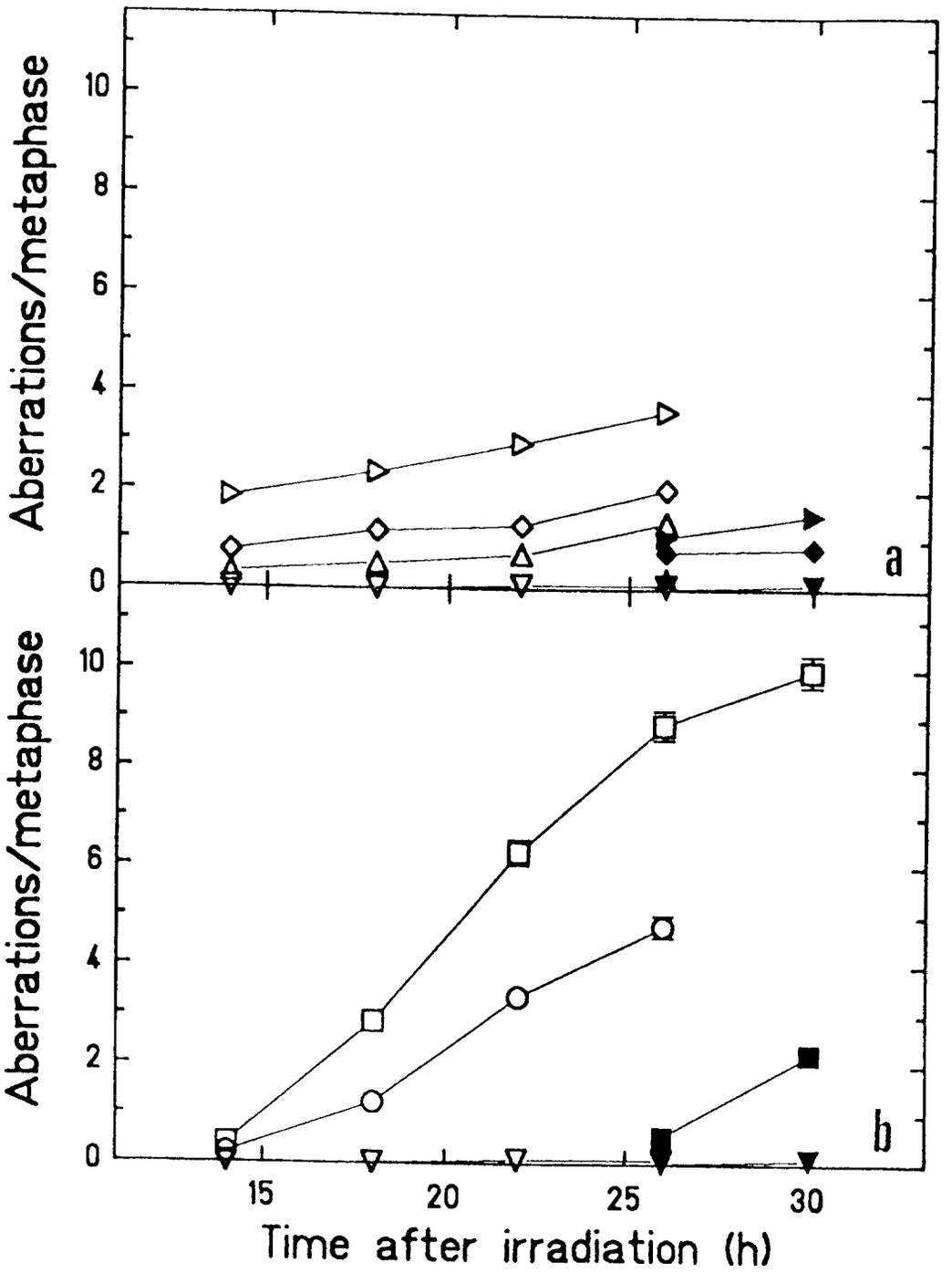

Fig. 3
Amount of aberrations per cell observed in first and second cycle meyaphases analyzed at different time intervals after the exposure to (a) X-rays or (b) Ar ions. The aberration types are specified in table 1. Key as in figure 2. If absent error bars are too small to be shown.

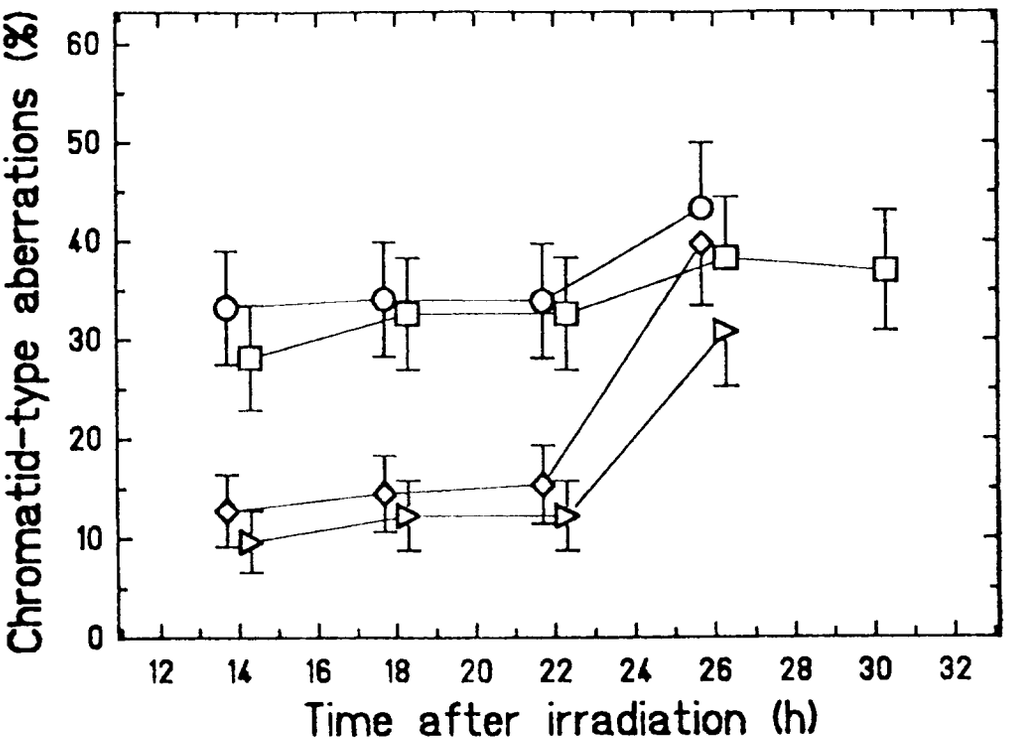

Fig.4
Percentage of chromatid-type aberrations (chromatid-type breaks and chromatid exchanges) among the total number of aberrations in first generation mitoses. Key as in figure 2.

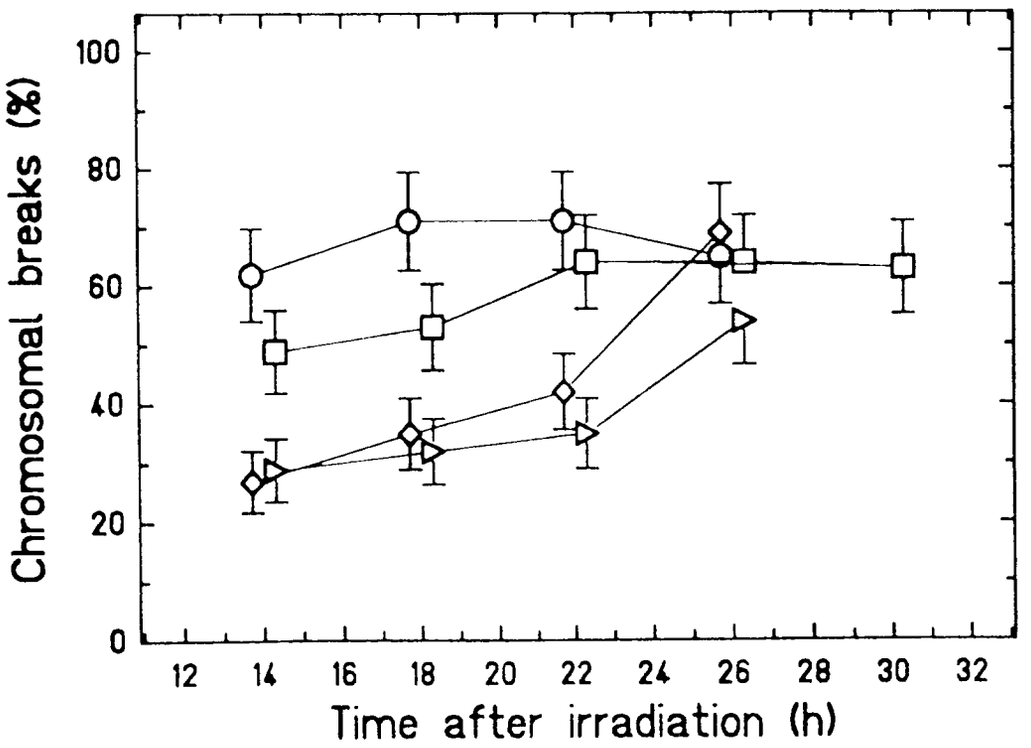

Fig. 5
Fraction of chromosomal breaks (chromosome- and chromatid-type breaks) among the total number of aberrations in first postirradiation mitoses after X-ray and Ar ion exposure. Key as in figure 2.

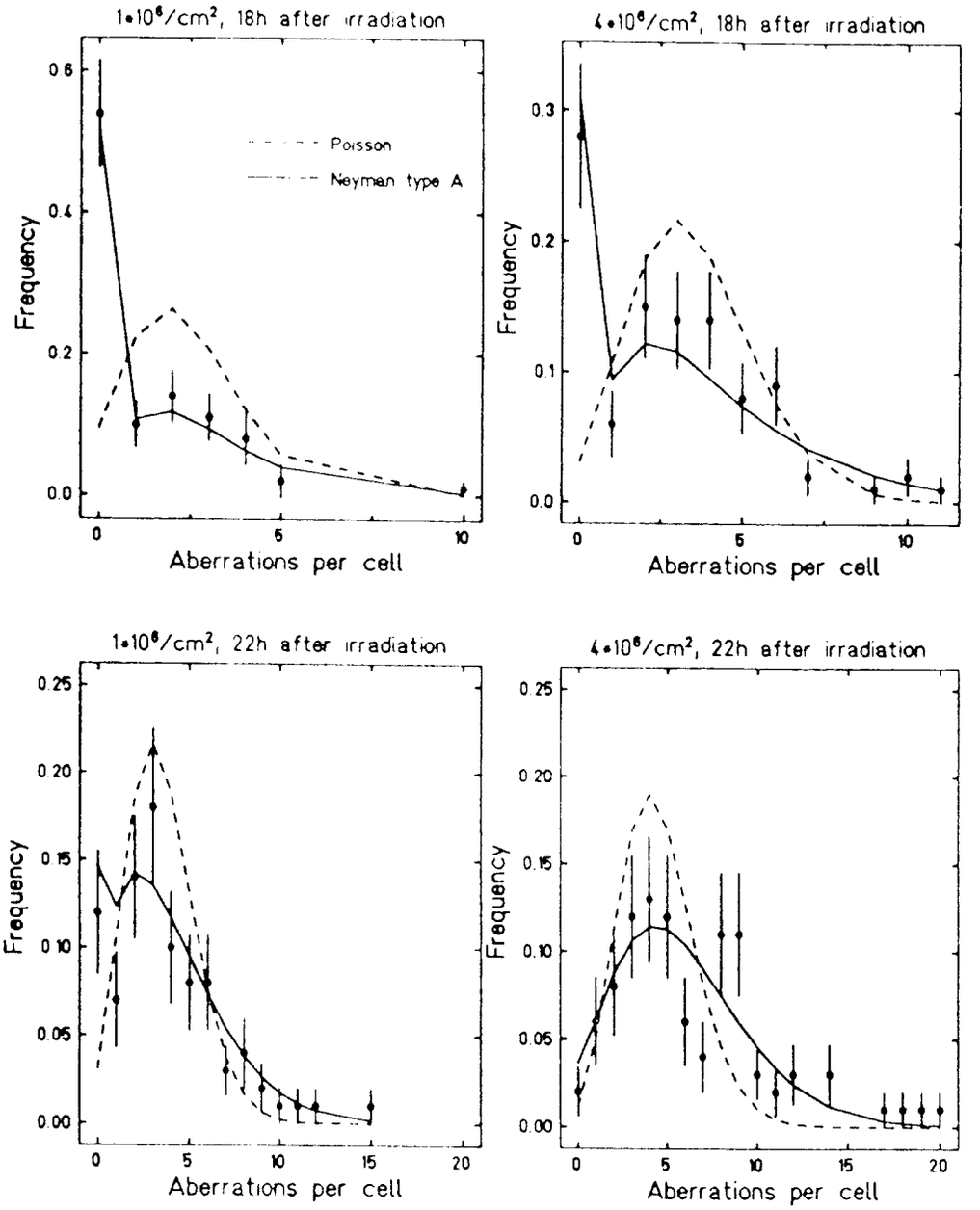

Fig. 6
Relative frequencies of aberrations/first cycle metaphase observed 14 and 22 hours after irradiation with 1×10^6 and 4×10^6 Ar ions (right panel). The dotted line shows the best fit to the data by Poisson distribution the solid line by Neyman Type A distribution. Vertical bars represent statistical errors determined by $\sqrt{n}$, if n is the frequency under consideration.

First cycle cells

Fixation time	Irradiation	Mitotic index (%)	Metaphases at 1st cycle (%)	Aberrant metaphases (%)	Aberration types						Number of aberrations
					csb	ctb	dmin	dic	r	cte	
14 h	Control	14,8	100,0	2	1	1	0	0	0	0	2
	X-ray 2 Gy	12,8	100,0	28	11	14	1	6	0	1	33
	4 Gy	9,7	100,0	48	12	9	26	21	7	3	77
	7 Gy	5,7	100,0	78	41	12	50	60	17	7	187
	Ar 1 x 10^6	5,2	100,0	14	8	5	5	1	0	2	21
	4 x 10^6	1,4	100,0	19	12	7	7	7	2	4	39
18 h	Control	6,2	100,0	2	0	2	0	0	0	0	2
	X-ray 2 Gy	12,8	100,0	38	17	6	14	9	3	3	52
	4 Gy	16,7	100,0	59	41	17	19	32	9	0	118
	7 Gy	17,3	100,0	89	50	24	74	66	16	7	237
	Ar 1 x 10^6	7,9	100,0	46	49	38	13	12	7	4	123
	4 x 10^6	6,4	100,0	72	74	74	65	48	7	18	286
22 h	Control	2,1	97,1	4	2	7	0	0	0	0	9
	X-ray 2 Gy	4,0	100,0	47	24	21	8	11	4	3	71
	4 Gy	2,8	100,0	73	37	17	27	39	7	3	130
	7 Gy	4,3	100,0	97	74	29	86	87	13	7	296
	Ar 1 x 10^6	4,3	100,0	78	137	101	50	29	6	14	337
	4 x 10^6	5,9	100,0	98	239	158	100	60	25	46	628
26 h	Control	6,2	3,9	7	4	5	0	0	0	0	9
	X-ray 2 Gy	3,4	13,4	60	38	65	7	18	4	5	137
	4 Gy	2,1	21,0	80	64	76	17	34	8	5	204
	7 Gy	1,9	36,8	97	100	95	63	76	11	17	362
	Ar 1 x 10^6	10,3	11,5	89	148	163	67	40	16	46	480
	4 x 10^6	7,8	53,9	100	283	281	191	56	18	58	887
30 h	Ar 4 x 10^6	7,3	19,7	100	325	300	221	69	14	68	997

Second cycle cells

Fixation time	Irradiation	Mitotic index (%)	Metaphases at 1st cycle (%)	Aberrant metaphases (%)	Aberration types						Number of aberrations
					csb	ctb	dmin	dic	r	cte	
26 h	Control	6,2	96,1	3	1	1	0	0	0	1	3
	X-ray 2 Gy	3,4	86,6	20	3	10	1	8	1	1	24
	4 Gy	2,1	79,0	44	10	29	14	18	5	1	77
	7 Gy	1,9	63,2	58	17	25	23	36	6	1	108
	Ar 1 x 10^6	10,5	88,5	30	5	28	10	8	0	0	51
	4 x 10^6	7,8	46,1	35	9	22	12	9	2	2	56
30 h	Control	6,2	99,2	10	0	11	0	0	0	0	11
	X-ray 4 Gy	6,8	98,4	54	34	24	10	13	2	2	85
	7 Gy	6,7	97,7	69	44	39	23	35	11	0	152
	Ar 4 x 10^6	7,3	80,3	76	73	30	53	51	13	3	223

Tab. 1
Frequency of chromosome aberrations and the corresponding mitotic index for several colcemid collection intervals after irradiation of V79 G_1-phase cells with X-rays or Ar ions.
Metaphases were stained with the FPG-technique to differentiate between cells in the first and second postirradiation cycle. Data for first cycle metaphases are given in table 1a, and for second cycle cells in table 1b. The abbreviated terms used are in agreement with the international nomenclature (ISCN 1978): csb (chromosome break), ctb (chromatid break), dmin (double minute), dic (dicentric chromosome), r (ring chromosome), cte (chromatid exchange).

Time [h]	Fluence $10^6/cm^2$	Poisson				Neyman Type A					
		$\bar{n}$	$\Delta\bar{n}$	χ^2	P	$\bar{n_1}$	$\Delta\bar{n_1}$	$\bar{n_2}$	$\Delta\bar{n_2}$	χ^2	P
14	1	0.14	0.04	0.59	0.61	0.68	0.79	0.23	0.29	0.50	0.60
18	1	2.35	0.17	12.49	$3.9\ 10^{-14}$	0.76	0.14	1.98	0.39	0.43	0.83
22	1	3.48	0.17	2.16	$8.8\ 10^{-3}$	2.49	0.45	1.47	0.27	0.89	0.55
26	1	4.87	0.23	1.86	0.029	2.43	0.41	2.10	0.35	0.99	0.45
14	4	0.14	0.04	2.38	0.05	0.29	0.09	1.15	0.48	1.09	0.35
18	4	3.48	0.18	3.89	$2.6\ 10^{-5}$	1.30	0.19	2.28	0.31	1.06	0.39
22	4	4.49	0.21	2.54	$6.2\ 10^{-4}$	4.64	0.95	1.26	0.29	1.28	0.19
26	4	7.57	0.30	2.01	$5.7\ 10^{-3}$	6.48	1.71	1.38	0.38	0.68	0.83

Tab. 2
Parameters for the frequency distribution of aberrations per first cycle cell fitted according to the Poisson and Neyman type A distribution, respectively. Parameters are described in the text. Reduced χ^2-values per degree freedom are given; P is the probability to find a higher χ^2 -value.